Journal of Medicinal Chemistry

Article

pubs.acs.org/jmc

Discovery of PG545: A Highly Potent and Simultaneous Inhibitor of Angiogenesis, Tumor Growth, and Metastasis

Vito Ferro,*[,†,§] Ligong Liu,[†,∥] Ken D. Johnstone,[†,⊥] Norbert Wimmer,[†,#] Tomislav Karoli,[†,∥] Paul Handley,[†] Jessica Rowley,[†] Keith Dredge,[†] Cai Ping Li,[†,∞] Edward Hammond,[†] Kat Davis,[†] Laura Sarimaa,[†,¶] Job Harenberg,[‡] and Ian Bytheway[†]

[†]Drug Design Group, Progen Pharmaceuticals Limited, Brisbane, Queensland 4076, Australia

[‡]Clinical Pharmacology, Faculty of Medicine Mannheim, Ruprecht-Karls University of Heidelberg, Mannheim, Germany

Supporting Information

ABSTRACT: Increasing the aglycone lipophilicity of a series of polysulfated oligosaccharide glycoside heparan sulfate (HS) mimetics via attachment of a steroid or long chain alkyl group resulted in compounds with significantly improved in vitro and ex vivo antiangiogenic activity. The compounds potently inhibited heparanase and HS-binding angiogenic growth factors and displayed improved antitumor and antimetastatic activity in vivo compared with the earlier series. Preliminary pharmacokinetic analyses also revealed significant increases in half-life following iv dosing, ultimately supporting less frequent dosing regimens in preclinical tumor models compared with other HS mimetics. The compounds also displayed only mild anticoagulant activity, a common side effect usually associated with HS mimetics. These efforts led to the identification of 3β-cholestanyl 2,3,4,6-tetra-*O*-sulfo-α-D-glucopyranosyl-(1→4)-2,3,6-tri-*O*-sulfo-α-D-glucopyranosyl-(1→4)-2,3,6-tri-*O*-sulfo-α-D-glucopyranosyl-(1→4)-2,3,6-tri-*O*-sulfo-β-D-glucopyranoside, tridecasodium salt (PG545, **18**) as a clinical candidate. Compound **18** was recently evaluated in a phase I clinical trial in cancer patients.

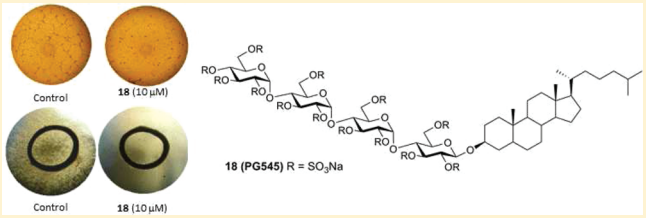

INTRODUCTION

Angiogenesis, the growth of new blood vessels from the pre-existing vasculature, is a critical process in tumor development, and its inhibition is now a well-established strategy for the treatment of cancer.[1,2] Recently approved antiangiogenic therapies include the anti-VEGF antibody bevacizumab and various tyrosine kinase inhibitors (TKIs).[3] While clinical antitumor effects are evident, overall survival benefits to patients have been relatively modest and a relapse to progressive disease often ensues,[4] possibly because the cancers utilize alternative angiogenic mechanisms.[5] More disturbingly, recent studies in mice have shown that treatment with some TKIs may result in a more aggressive phenotype and may promote metastases in some circumstances.[6−8] Additionally, many of the currently approved antiangiogenic therapies are associated with cardiotoxic side effects.[9] The development of new angiogenesis inhibitors with fewer side effects that target multiple proangiogenic factors and also inhibit metastasis is therefore a worthwhile strategy to provide improved survival outcomes in cancer patients.

An example of the above approach is the use of heparan sulfate (HS) mimetics to simultaneously block HS-mediated growth factor signaling leading to angiogenesis[10] and to inhibit heparanase,[11,12] an endo-β-glucuronidase that cleaves HS and facilitates metastasis. Of particular note is muparfostat (also known as PI-88, **1**, Chart 1),[13] a complex mixture of sulfated oligosaccharides with antiangiogenic and antimetastatic activity that is currently in phase III clinical trials for post-resection hepatocellular carcinoma.[14,15] Recently we described[16] the synthesis and evaluation as angiogenesis inhibitors of a series of polysulfated penta- and tetrasaccharide glycosides containing the $\alpha(1\rightarrow3)/\alpha(1\rightarrow2)$-linked mannose sequence found in **1**. Compared with other HS mimetics, these compounds are stable, fully sulfated, single chemical entities. These compounds strongly inhibited heparanase and displayed potent activity in cell-based and ex vivo angiogenesis assays, with tetramannosides showing activity comparable to that of pentamannosides. Selected compounds (e.g., **2** and **3**) also showed good antitumor activity in vivo in a mouse melanoma (solid tumor) model resistant to **1**. Furthermore, the lipophilic modifications resulted in reduced anticoagulant activity, a common side effect of HS mimetics,[17] and conferred a reasonable pharmacokinetic profile in the rat, thus building on earlier results.[18,19] These data supported the further investigation of this class of compound as potential antiangiogenic, anticancer therapeutics. Herein we describe the extension of these studies to compounds with larger, more lipophilic aglycones and with alternative saccharide backbones. We show that these modifications endow the compounds with more potent antiangiogenic activity and improved pharmacokinetics, which have subsequently translated into significantly

Received: December 19, 2011
Published: March 29, 2012

Chart 1. Structures of Oligomannoside HS Mimetics[a]

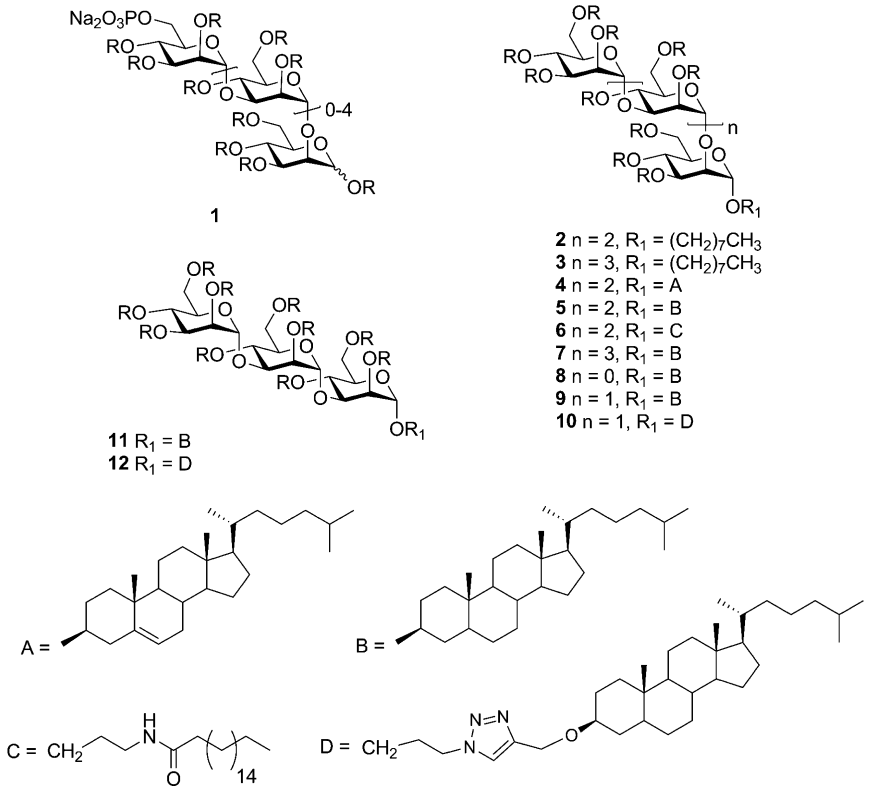

[a]R = SO_3Na.

Scheme 1[a]

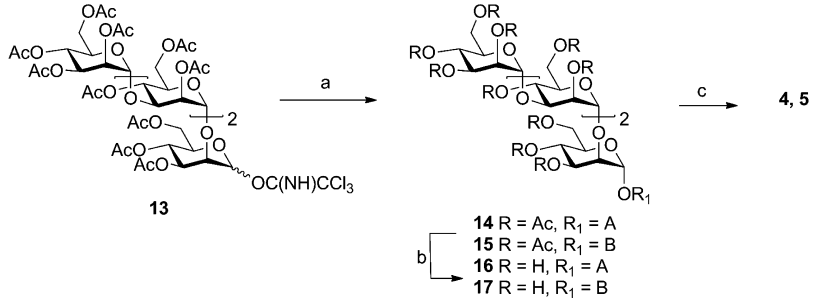

[a]Reagents and conditions: (a) cholesterol or cholestanol, TMSOTf, DCM, 0 °C; (b) (i) NaOMe/MeOH; (ii) AG-50W-X8 (H^+ form); (c) (i) SO_3·Py, DMF, 60 °C; (ii) Na_2CO_3 (aq). For structures of aglycones **A** and **B**, see Chart 1.

greater potency in in vivo models and ultimately resulted in the selection of a clinical candidate.

RESULTS AND DISCUSSION

We reasoned that significantly increasing the lipophilicity of the aglycone in this class of compound could result in increased membrane and protein binding leading to increases in plasma residence time and potency. In the earlier study[16] the dodecyl group gave no clear benefit over the shorter octyl group. The first compounds targeted for synthesis were therefore the significantly more lipophilic steroidal tetramannosides **4** and **5**, which were prepared according to Scheme 1. Glycosylation of cholesterol or cholestanol with trichloracetimidate **13**[16] using TMSOTf as the promoter gave exclusively the α-linked glycosides **14** and **15** in moderate yield. Deprotection (NaOMe in MeOH) followed by exhaustive sulfonation (excess SO_3·Py, DMF, 60 °C) gave the target compounds **4** and **5** in moderate yield (42−44%). Sulfonation of **16** gave a mixture of products by CE,[20] presumably due to the relative instability of the cholesteryl group to the sulfonation conditions, requiring purification by size exclusion chromatography. However, sulfonation of cholestanyl glycoside **17** proceeded smoothly to give **5** in >95% purity by CE following simple purification by dialysis. Cholestanol was thus used as the steroidal glycosyl acceptor of choice for subsequent compounds.

Compound **5** bound tightly to the angiogenic growth factors FGF-1, FGF-2, and VEGF (K_i in the low nanomolar to picomolar range, Table 1) as determined by a surface plasmon resonance-based solution affinity assay[21,22] and potently inhibited heparanase activity[23] (K_i = 5.8 nM, Table 2),[24] indicating that the larger aglycone did not adversely affect activity. When tested in growth factor-induced endothelial cell proliferation assays[25] using HUVECs (Table 2), compound **5** displayed significantly improved potency compared with the

dx.doi.org/10.1021/jm201708h | J. Med. Chem. 2012, 55, 3804−3813

Table 1. Growth Factor Binding of Test Compounds[a]

compd	K_d (nM) FGF-1	FGF-2	VEGF
1[b]	0.24 ± 0.04	61 ± 9	2.2 ± 2.3
2[b]	0.118 ± 0.009	160 ± 40	18 ± 5
5	0.60 ± 0.50	160 ± 40	22 ± 6
6	0.44 ± 0.04	108 ± 11	40 ± 17
7	0.24 ± 0.10	39 ± 6	1.04 ± 0.19
8	270 ± 30	1570 ± 150	1300 ± 300
9	18.5 ± 1.8	631 ± 4	319 ± 19
10	22.6 ± 1.0	480 ± 40	460 ± 30
11	16 ± 7	490 ± 40	90 ± 30
12	14.3 ± 3.0	474.0 ± 1.4	260 ± 130
18	8 ± 4	390 ± 80	28.9 ± 2.3
19	9.7 ± 0.8	390 ± 90	95 ± 8
20	50 ± 8	610 ± 60	790 ± 230
21	1.25 ± 0.07	50 ± 4	7.95 ± 0.07
22	24.8 ± 2.3	547 ± 50	190 ± 60
23	4.94 ± 0.08	311 ± 25	14 ± 4
24	32.2 ± 2.3	530 ± 50	380 ± 110
25	560 ± 30	2200 ± 400	1200 ± 400
26	840 ± 130	3400 ± 300	1930 ± 230
27	3600 ± 600	>3000	3000 ± 400
28	870 ± 60	2000 ± 400	1350 ± 70
29	610 ± 210	1800 ± 300	1600 ± 300

[a]Binding affinities for growth factors FGF-1, FGF-2, and VEGF were determined using a surface plasmon resonance-based solution affinity assay, as previously described.[21,22] The K_d values represent the average of at least duplicate measurements ± the standard deviation. [b]Data from Johnstone et al.[16]

earlier series (e.g., the octyl tetramannoside **2**) for all growth factors tested (FGF-1, FGF-2, and VEGF). The IC_{50} values were approximately 10-fold (for FGF-2) or 6-fold (for FGF-1 and VEGF) lower compared with the corresponding values for **2**. A series of analogues of **5** were then synthesized, initially based on the same oligomannose scaffold in **2** while varying the length and linkage of the oligosaccharide. We were particularly interested to see if the increased lipophilicity could improve the potency of shorter oligosaccharides, as similar compounds had previously possessed only modest HS-mimetic activity compared with longer congeners.[13,26] The introduction of a spacer between the saccharide and the cholestanol was also investigated, as was the use of an alternative highly lipophilic aglycone, 3-stearamidopropyl. Compounds **6**−**12** were prepared in a manner similar to that shown in Scheme 1 via glycosylation, deprotection, and sulfonation. The compounds with a triazole spacer (**10**, **12**) were prepared via the Cu(I)-catalyzed Huisgen 1,3-dipolar cycloaddition ("click") reaction[27,28] between the protected azidopropyl glycoside and 3β-*O*-(prop-2-ynyl)cholestanol. Reduction of the azide group (Ph_3P) followed by coupling with stearyl chloride furnished the stearamidopropyl derivative **6**.

Previous studies of sulfated oligosaccharides as HS mimetics have shown that activity is dependent on monosaccharide composition as well as on the length and linkage of the oligosaccharide.[13,17,26] Therefore, we also investigated HS mimetics with alternative monosaccharides to D-mannose. Particular attention was focused toward $\alpha(1\rightarrow4)$-linked oligosaccharides of D-glucose (i.e., maltosaccharides) because when exhaustively sulfonated, these compounds show potent antiangiogenic and anti-heparanase activity similar to that of the $\alpha(1\rightarrow3)/\alpha(1\rightarrow2)$-linked mannose oligosaccharides. Polysulfated maltohexaose, for example, displays similar potency to **1** in in vitro angiogenesis and heparanase inhibition assays.[13] In addition, maltosaccharides are commercially available and inexpensive, being important products in the starch industry. The corresponding polysulfated oligomaltosides should thus be cheaper to manufacture than the oligomannosides where the starting oligosaccharide must first be synthesized from monosaccharide building blocks.[26,29] Compounds **18**−**29** (Chart 2) were prepared similarly according to Scheme 1 via TMSOTf-catalyzed reaction of peracetylated or perbenzoylated trichloroacetimidate glycosyl donors with cholestanol or with 3-azidopropanol followed by reduction and coupling with stearyl chloride. The use of participating protecting groups (acetyl or benzoyl) gave the expected β-linked glycosides as the sole glycosylation products. In this series, cholestanol conjugates with a triazole linker were synthesized via the click reaction between 3β-*O*-(prop-2-ynyl)cholestanol and the corresponding protected β-glycosyl azides, which were themselves readily prepared from the corresponding α-glycosyl bromides by nucleophilic displacement with azide ion (see Supporting Information). The maltotetraosyl azide also provided access to conjugate **21** in which the steroid (deoxycholic acid) was attached with the opposite orientation, via reduction to the glycosylamine (H_2, 10% Pd/C) and HOBt-mediated coupling with diacetyldeoxycholic acid.[30]

All test compounds were of ≥95% purity by CE following purification by dialysis, and ^1H and ^{13}C NMR data were consistent with full sulfonation, as noted for the earlier series.[16] The compounds were evaluated for their ability to inhibit heparanase, bind to angiogenic growth factors, and inhibit growth factor-induced endothelial cell proliferation (Tables 1 and 2). The anticoagulant activity of the compounds was also determined via the APTT and Heptest assays (Table 2), and selected compounds were evaluated in the Matrigel microtubule formation assay and the ex vivo rat aortic angiogenesis assay (Figure 1).

As seen with the earlier series,[16] the presence of a lipophilic aglycone significantly attenuated the anticoagulant activity of the compounds compared with nonglycosylated **1**. The data also indicate that compounds with either a stearamidopropyl or cholestanyl group, with or without a spacer, had strong affinities for the angiogenic growth factors FGF-1, FGF-2, and VEGF, with tetrasaccharides displaying K_d values similar to those of their less lipophilic congeners from the earlier series.[16] It was also evident that affinity (particularly for VEGF and FGF-1) was, not unexpectedly, dependent on oligosaccharide chain length; e.g., compared with maltotetraoside **18**, the affinity of maltotrioside **22** for VEGF and FGF-1 was 6-fold and 3-fold lower, whereas for maltoside **25** the affinity was 40-fold and 70-fold lower, respectively. Interestingly, however, heparanase inhibitory activity was significantly improved. Sulfated di- and trisaccharides with small or no aglycones display only partial competitive inhibition of heparanase[26] and do not completely inhibit the enzyme even at very high concentrations, presumably because substrate access to the enzyme active site is not completely blocked. For example, a sulfated mannobiose only inhibited heparanase up to 58.6% with an IC_{50} of 1.57 ± 0.31 μM (K_{ic} = 2.23 ± 0.20 μM; K_{iu} = 68.3 ± 22.4 μM).[26] In contrast, all the compounds in this series completely inhibited heparanase activity with the maltotrioside **22** showing activity comparable to that of the maltotetraoside **18** (K_i of 9 and 6 nM,

dx.doi.org/10.1021/jm201708h | J. Med. Chem. 2012, 55, 3804−3813

Table 2. Inhibition of Growth Factor-Induced HUVEC Proliferation,[a] Inhibition of Heparanase,[b] and Anticoagulant Activity (at 0.1 mg/mL)[c] of Test Compounds

	IC_{50} (μM)				anticoagulant activity	
compd	FGF-1	FGF-2	VEGF	K_i (nM) heparanase	APTT (s)	Heptest (s)
1[d]	42 ± 14	10 ± 5	20 ± 6	7.9 ± 0.6[e]	>500	>500
2[d]	9 ± 2	9 ± 2	9 ± 5	59 ± 7	96.7	79.5
5	1.29 ± 0.25	0.80 ± 0.30	1.2 ± 1.0	5.8 ± 1.5	94.0	28.0
6	1.54 ± 0.16	0.70 ± 0.30	0.60 ± 0.60	6.0 ± 2.1	68.1	24.5
7	0.99 ± 0.10	0.39 ± 0.07	0.22 ± 0.16	5.5 ± 2.6	63.3	29.6
8	>10	2.22 ± 0.22	1.8 ± 1.1	22.3 ± 1.6	40.6	25.5
9	4.4 ± 0.5	2.27 ± 0.23	1.0 ± 0.5	6.4 ± 2.5	50.7	27.3
10	3.8 ± 0.6	1.7 ± 0.4	2.1 ± 1.9	8.50 ± 0.14	73.3	33.1
11	2.5 ± 0.7	1.8 ± 1.0	1.7 ± 1.2	10.5 ± 1.7	58.5	24.2
12	2.61 ± 0.14	1.2 ± 0.4	1.4 ± 1.1	8.4 ± 2.6	71.4	26.4
18	1.21 ± 0.17	0.70 ± 0.30	0.5 ± 0.3	6.1 ± 2.5	71.9	28.6
19	2.3 ± 1.1	0.64 ± 0.27	2.2 ± 0.9	3.7 ± 0.8	104.0	45.5
20	2.1 ± 0.6	1.2 ± 0.3	1.8 ± 0.6	16 ± 4	61.2	30.2
21	>50.0	>50.0	>50.0	20 ± 5	41.0	26.8
22	2.5 ± 1.4	2.3 ± 1.2	1.6 ± 0.6	9.1 ± 2.5	51.6	29.2
23	0.47 ± 0.23	0.80 ± 0.50	0.24 ± 0.16	9.1 ± 0.3	65.8	32.2
24	1.7 ± 0.8	1.7 ± 1.3	1.1 ± 0.6	11.3 ± 0.4	51.1	24.9
25	4.0 ± 1.5	>10	5.2 ± 2.4	ND[f]	38.6	23.9
26	4.1 ± 0.9	4.17 ± 0.08	1.13 ± 0.19	ND[f]	40.3	26.7
27	2.2 ± 0.4	2.9 ± 0.4	2.24 ± 0.22	111 ± 28	36.1	23.9
28	6 ± 3	5.6 ± 0.5	5.6 ± 1.5	ND[f]	38.8	25.3
29	2.7 ± 0.4	2.43 ± 0.12	2.62 ± 0.17	30 ± 7	39.6	25.3

[a]The IC_{50} data represent the mean and SD where compounds were tested in two to eight independent experiments. Data without SD are from single experiments. [b]K_i ± the standard error determined from inhibition response curves as previously described.[23] [c]APTT and Heptest values are the mean values of two determinations. The normal ranges for coagulation values in pooled human plasma are 26−36 s for APTT and 13−20 s for heptest. [d]Data from Johnstone et al.[16] [e]Data from Hammond et al.[23] [f]Not determined.

Chart 2. Structures of HS Mimetics[a]

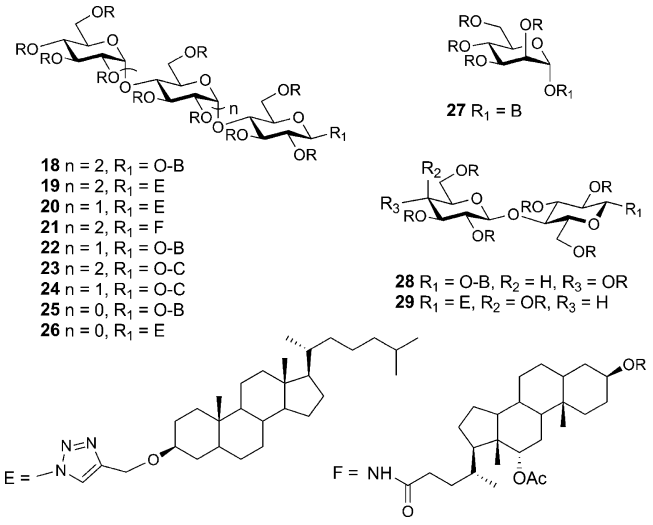

[a]R = SO_3Na. For structures of aglycones **B**−**D**, see Chart 1.

respectively) and with even the mannobioside **8** and mannoside **27** showing good activity (K_i of 22 and 111 nM, respectively).

The nature of the oligosaccharide backbone had an interesting effect on growth factor affinity. For example, while the mannotetraoside **5** and maltotetraoside **18** had the same inhibitory potency against heparanase and a similar affinity for VEGF, **5** had a 13-fold greater affinity for FGF-1 and a 2.5-fold greater affinity for FGF-2 than **18**. These results reinforce the view that different sulfated oligosaccharides have unique spatial and conformational requirements for binding to HS-binding proteins beyond simply chain length and charge density.[31]

The increased potency of the new compounds compared with **1** and the earlier series became apparent in cell-based assays used to determine antiangiogenic activity. We attribute this increased potency to improved bioavailability, possibly because of better localization to the cell surface membrane by the lipophilic aglycone. Our results indicate that the stearamidopropyl and cholestanyl aglycones have similar effects in this regard. The first of these assays focuses on the compounds' ability to inhibit endothelial cell proliferation in response to angiogenic growth factors (Table 2). With one exception, all compounds potently inhibited FGF-1-, FGF-2-, and VEGF-induced proliferation of HUVECs (Table 2), with IC_{50} values up to 28-fold (for FGF-2) or 90-fold (for FGF-1 and VEGF) lower compared with **1** and 25-fold (for FGF-2), 19-fold (for FGF-1), or 40-fold (for VEGF) compared with **2**. The exception was compound **21**, with a sulfo group at the aglycone (deoxycholic acid) terminus, which had no inhibitory activity up to 50 μM, presumably because the sulfo group reduced the overall lipophilicity of the aglycone. The potency in cell proliferation assays produced similar trends with respect to oligosaccharide chain length, as seen in growth factor binding assays, although the magnitude of the differences was smaller and dependent on the growth factor. For example, in the homologous series **25**, **22**, and **18** for VEGF the IC_{50} increases 10-fold (0.5−5 μM), for FGF-2 the increase is >10-fold (0.7 to >10 μM), while for FGF-1 the increase is only ∼4-fold (1.2−4 μM). Similar results and trends for all compounds were also

dx.doi.org/10.1021/jm201708h | J. Med. Chem. 2012, 55, 3804−3813

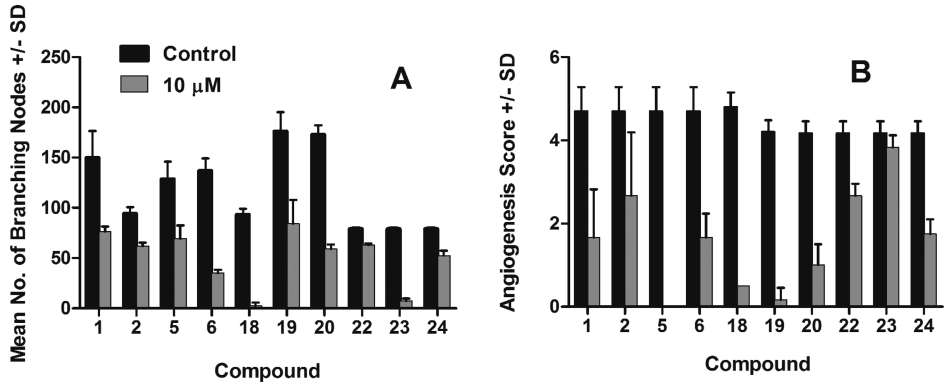

Figure 1. Inhibition of in vitro and ex vivo angiogenesis by test compounds at 10 μM. (A) Inhibition of HUVEC tube formation. Tube formation was assessed using low magnification (×40) and counting the total number of branching nodes connecting three or more tubules. Data are presented as the mean number of branching nodes ± SD compared with controls. (B) Inhibition of microvessel outgrowths in the rat aortic assay, determined using a scoring system outlined in the Experimental Section.

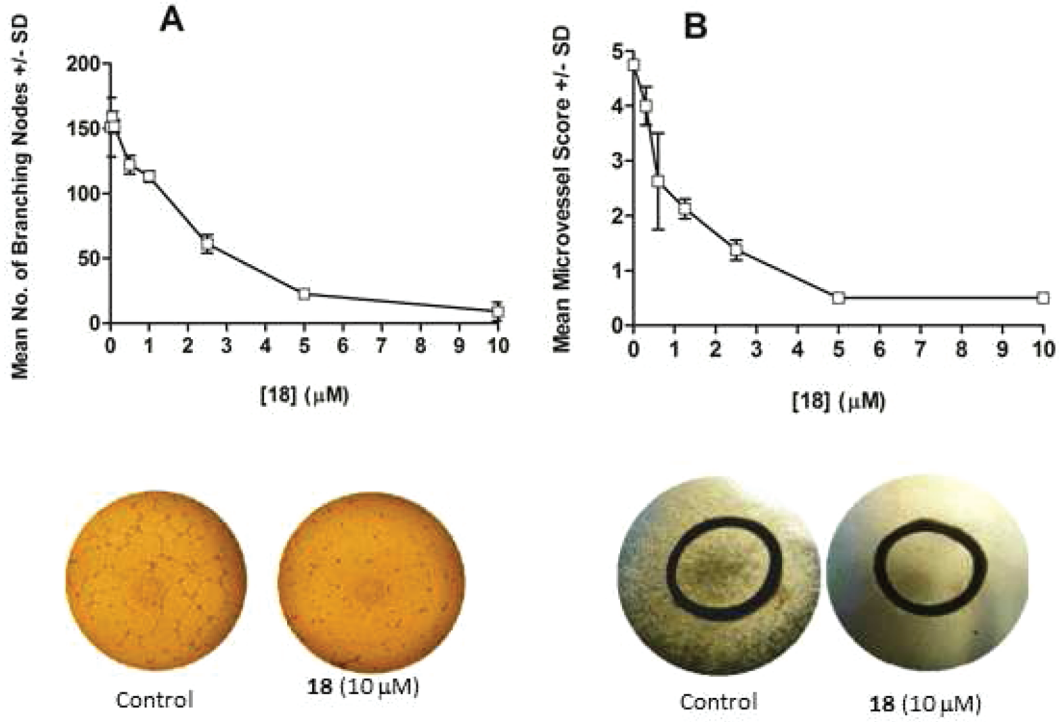

Figure 2. Dose related inhibition of in vitro and ex vivo angiogenesis by **18**. (A) Dose related effect of **18** on capillary tube formation of dHMVECs after 18 h of incubation on Matrigel basement membrane. Values are shown as mean number of branching nodes ± SD. Representative images of control and **18** (10 μM) are also shown below. (B) Dose related antiangiogenic effect of increasing concentrations of **18** in Matrigel cultures of rat aortic ring explants maintained in the absence of exogenous growth factors. Values are the mean ± SD of microvessel outgrowths after daily treatment for 6 days. Representative images of control and **18** (10 μM) are also shown below.

obtained using dermal human microvascular endothelial cells (dHMVECs) in place of HUVECs (data not shown).

Endothelial cell tube formation on Matrigel using HUVECs (or dHMVECs) was also strongly inhibited, with some compounds (i.e., **5**, **6**, **18**, and **23**) showing >80% inhibition at 10 μM (Figure 1A), a significant improvement compared with **1** and **2**.[16] Selected compounds were also evaluated in the ex vivo rat aortic angiogenesis assay (Figure 1B) with compounds **5**, **18**, and **19** emerging as the most potent, all inhibiting angiogenesis by over 80% when administered daily at 10 μM for 6–8 days.[25] The rat aorta assay is considered to come closer to simulating the in vivo situation not only because it includes the surrounding nonendothelial cells but also because the endothelial cells have not been preselected by passaging and are thus not in a proliferative state at the time of explantation.[32] This may account for the fact that some compounds were more potent in one assay over the other. Figure 2 shows representative dose response data for **18** (ultimately selected as a clinical candidate; see below), which indicates that it is a potent inhibitor of in vitro and ex vivo angiogenesis with IC_{50} values of 2.0 ± 0.5 μM and 1.1 ± 0.2 μM, respectively, for the tube formation and rat aorta assays, respectively. It is important to note that the compounds were not cytotoxic at the inhibition values (IC_{50} and K_d/K_i) in the above assays, e.g., the LC_{50} for **18** (78 μM)[25] is approximately 80-fold higher than its IC_{50} in the cell proliferation assay. In

dx.doi.org/10.1021/jm201708h | J. Med. Chem. 2012, 55, 3804–3813

experiments to assess tissue viability following 6 days of treatment with the test compounds, aortic segments receiving fresh medium containing VEGF (10 ng/mL) frequently developed new microvessels within 72 h (data not shown), confirming the lack of cytotoxicity.

Several compounds including **18**−**20** and **22**−**24** were then evaluated in syngeneic murine models of tumor growth and metastasis, the B16 melanoma model and the B16 experimental metastasis model. When administered by subcutaneous injection as solutions in PBS for 12 consecutive days at a dose of 10 mg/kg, compounds **18**−**20** potently inhibited the development of metastatic nodules.[25] In the B16 solid tumor model, a model that is resistant to treatment with compound **1**, daily administration of compounds **18**−**20** at 15 mg/kg for 12 days, 3 days after tumor challenge, resulted in potent inhibition of tumor growth with no evidence of palpable tumors until cessation of drug treatment.[25] This compares favorably with the earlier series (e.g., **2**, **3**) where palpable tumors were evident after several days of treatment at 30 mg/kg (b.i.d.). Compound **18** was also shown to significantly inhibit tumor growth in the HT29 colon xenograft model when administered daily at 5 mg/kg.[25]

Preliminary screening pharmacokinetic evaluation of compounds **18**−**20** and **22**−**24** indicated that the more lipophilic aglycones were indeed significantly affecting their pharmacokinetic properties, with apparent half-lives in the rat at least >3-fold longer than for the octyl tetrasaccharide **2** (see Supporting Information), presumably as a result of increased binding to lipophilic cell membranes and plasma proteins. Subsequent detailed pharmacokinetic analyses of **18** revealed that it has a relatively long half-life. For example, the mean elimination half-life of [^{3}H]-labeled **18** in tumor-bearing mice was >50 h following up to three sc bolus doses at 96 h intervals.[33] The long half-life of **18** enabled less frequent dosing regimens (e.g., weekly or twice weekly) in preclinical models while maintaining substantial efficacy.[33]

The above studies, in combination with considerations such as manufacturability and pharmacokinetic properties (see below), ultimately resulted in the selection of compound **18** as the clinical candidate. Compound **18** was subsequently subjected to extensive pharmacological evaluation in multiple preclinical models, as detailed elsewhere.[33] In summary, **18** was shown to potently inhibit angiogenesis in vivo and solid tumor growth in murine models of breast, prostate, liver, lung, colon, head and neck cancers and melanoma. Compound **18** also displayed potent antimetastatic activity in murine models of experimental and spontaneous metastasis and showed enhanced antitumor activity in a liver cancer model when used in combination with the TKI sorafenib.[33] It is important to note that sorafenib, an approved drug for kidney and liver cancer, showed no antimetastatic activity in these models.

In conclusion, further optimization of a series of polysulfated oligosaccharide glycosides via increasing the lipophilicity of the aglycone resulted in HS mimetics with potent and significantly improved in vitro and ex vivo antiangiogenic activity and in vivo antitumor and antimetastatic activity. Preliminary pharmacokinetic analyses also revealed significant increases in half-life following iv dosing, ultimately supporting less frequent dosing regimens compared with other HS mimetics.[33] The improved potency and pharmacokinetics may be because of better localization to the cell surface membrane by the lipophilic aglycone. The compounds displayed only mild anticoagulant activity, a common side effect usually associated with HS mimetics. Changing the oligosaccharide backbone from oligomannose to the cheaper and more readily accessible maltotetraose also resulted in compounds with improved manufacturability. These efforts led to the discovery of the clinical candidate **18** (PG545), which was recently evaluated in a phase I clinical trial in cancer patients. The antimetastatic activity of **18**, due to its potent inhibition of heparanase, differentiates it from other antiangiogenic agents such as the TKIs. In light of recent preclinical findings regarding anti-VEGF therapies, this attribute may be of critical importance as **18** progresses through the clinic.

EXPERIMENTAL SECTION

General Information. Unless otherwise stated, nuclear magnetic resonance (NMR) spectra were recorded at 400 MHz for ^{1}H and 100 MHz for ^{13}C, in either deuteriochloroform ($CDCl_3$) with residual $CHCl_3$ (^{1}H, δ 7.26) or deuterium oxide (D_2O), employing residual HOD (^{1}H, δ 4.78) as internal standard, at ambient temperatures (298 K). Where appropriate, analyses of ^{1}H NMR spectra were aided by gCOSY experiments. Flash chromatography was performed on silica gel (40−63 μm) under a positive pressure with specified eluants. All solvents used were of analytical grade. The progress of reactions was monitored by thin layer chromatography (TLC) using commercially prepared silica gel 60 F_{254} aluminum-backed plates. Compounds were visualized by charring with 5% sulfuric acid in methanol and/or under ultraviolet light. Analytical HPLC was performed on a Waters Alliance 2690 separations module equipped with a Waters 2410 refractive index detector, using a Phenomenex PolySep-GFC-P2000 (300 mm × 7.8 mm) column and 0.1 M $NaNO_3$ as the mobile phase. The flow rate was 0.8 mL/min, and the column temperature was set to 35 °C. Capillary electrophoresis (CE) was performed in reverse polarity mode on an Agilent CE system using 10 mM 5-sulfosalicylic acid, pH 3, as the background electrolyte and detection by indirect UV absorbance at 214 nm, as previously described.[20] Compound homogeneity was determined by ^{1}H and/or ^{13}C NMR spectroscopy and for the final products by CE and/or HPLC. Unless indicated otherwise, the purity of the final products was ≥95%.

2,3,4,6-Tetra-*O*-acetyl-α-D-glucopyranosyl-(1→4)-2,3,6-tri-*O*-acetyl-α-D-glucopyranosyl-(1→4)-2,3,6-tri-*O*-acetyl-α-D-glucopyranosyl-(1→4)-1,2,3,6-tetra-*O*-acetyl-D-glucopyranose (30). Dry maltotetraose (502 mg, 0.753 mmol) and DMAP (cat.) were dissolved in dry pyridine (10 mL) and cooled at 0 °C. A solution of Ac_2O (2.8 g, 27.4 mmol, 2.6 equiv per hydroxy group) in pyridine (5 mL) was added dropwise at 0 °C. The mixture was stirred at 0 °C for 4 h and left at −20 °C for 48 h. The reaction was not completed; therefore, additional Ac_2O (1.0 g, 9.8 mmol) was added at 0 °C. The mixture was stirred at room temperature for 16 h, cooled to 0 °C, and treated with dry MeOH (10 mL). After being stirred at room temperature for 2 h, the solution was concentrated and the residue coevaporated with toluene (3 × 30 mL) to give the peracetate **30** as a white solid (920 mg, 97%). ^{1}H and ^{13}C NMR spectra were in accord with the literature.[34]

2,3,4,6-Tetra-*O*-acetyl-α-D-glucopyranosyl-(1→4)-2,3,6-tri-*O*-acetyl-α-D-glucopyranosyl-(1→4)-2,3,6-tri-*O*-acetyl-α-D-glucopyranosyl-(1→4)-2,3,6-tri-*O*-acetyl-α-D-glucopyranosyl Trichloroacetimidate (31). To a precooled (0 °C) solution of ethylenediamine (1.66 mmol, 0.11 mL) in dry THF (15 mL) was added dropwise glacial acetic acid (0.90 mmol, 0.053 mL). A precipitate was formed immediately. The peracetate **30** (900 mg, 0.717 mmol) was added at 0 °C and the mixture stirred at room temperature for 2 h until TLC (toluene/EtOAc, 1:2) indicated the absence of the starting material and the presence of a slower moving product. The solution was neutralized using acetic acid (0.15 mL, to pH 6). The solvent was blown out with a stream of air. The residue was dissolved in EtOAc (100 mL), washed with saturated $NaHCO_3$ solution (3 × 50 mL), water (3 × 10 mL), brine (30 mL), and dried (Na_2SO_4). The solution was filtered and concentrated in vacuo to give the hemiacetal as a yellow foam (830 mg, 0.684 mmol), which was dissolved in dry DCM (5 mL). The solution was cooled to 0 °C, and

K_2CO_3 (1.20 g, 8.60 mmol) and trichloroacetonitrile (0.849 mL, 8.40 mmol) were added. The mixture was stirred at room temperature for 2 h. The mixture was purified by flash chromatography (silica gel, 20 cm × 1.5 cm, toluene−EtOAc, 1:2 → EtOAc, containing 0.2% (v/v) Et_3N) to give the desired trichloroacetimidate[34] **31** as a white fluffy powder (795 mg, 86%). The compound was dried over P_2O_5 overnight and stored at −20 °C.

3β-Cholestanyl 2,3,4,6-Tetra-*O*-acetyl-α-D-glucopyranosyl-(1→4)-2,3,6-tri-*O*-acetyl-α-D-glucopyranosyl-(1→4)-2,3,6-tri-*O*-acetyl-α-D-glucopyranosyl-(1→4)-2,3,6-tri-*O*-acetyl-β-D-glucopyranoside (32). The trichloroacetimidate **31** (300 mg, 0.221 mmol), cholestanol (2 equiv, 172 mg, 0.442 mmol), and 3 Å molecular sieves (100 mg) were stirred in dry DCM (1.5 mL) for 0.5 h. A solution of TMSOTf in dry DCM (0.4 M, 0.275 mL, 0.11 mmol, 0.5 equiv) was added dropwise at 0 °C. After 30 min at room temperature, another portion of TMSOTf in dry DCM (0.4 M, 0.2 mL, 0.08 mmol, 0.36 equiv) was added and stirring continued for 30 min at room temperature. The reaction was quenched by adding Et_3N (0.025 mL) at 0 °C. After being stirred for 10 min, the mixture was filtered through a plug of Celite (0.5 cm) and washed with DCM (5 × 25 mL) and EtOAc (3 × 25 mL). Both organic phases were washed separately with saturated $NaHCO_3$ solution (3 × 25 mL) and brine (25 mL). Aqueous extracts were combined and re-extracted with EtOAc (3 × 30 mL). The EtOAc extracts were combined and washed with brine (30 mL), combined with the other organic extracts and dried (Na_2SO_4). The solution was filtered and concentrated in vacuo to afford a yellow foam (480 mg). Flash chromatographic purification (silica gel, 30 cm × 5 cm, toluene/EtOAc, 3:2 → 1:1 → 1:2 → EtOAc, containing 0.2% Et_3N (v/v)) afforded two fractions. Fraction A gave the desired β-linked glycoside **32** as a white foam (81 mg, 23%), and fraction B contained 77% partially deacetylated α-linked glycoside and 23% partially deacetylated β-linked glycoside (118 mg). ^{1}H NMR ($CDCl_3$, 400 MHz): δ 5.24−5.45 (m, 7H, 3 × H1, 4 × H3), 5.08 (t, 1H, $J_{3,4}$ = $J_{4,5}$ = 9.80 Hz, H4^{IV}) 4.86 (dd, 1H, $J_{1,2}$ = 4.1, $J_{2,3}$ = 10.4, H2^{IV}), 4.70−4.80 (m, 3H, 3 × H2), 4.63 (d, 1H, $J_{1,2}$ = 7.7, H1^{I}), 4.33−4.54 (m, 4H, 4 × H6), 3.86−4.31 (m, 10 H, 3 × H4, 3 × H5, 4 × H6), 3.70 (ddd, 1H, H5^{I}), 3.56 (m, 1H, cholestanyl-H3), 2.20, 2.19, 2.16, 2.11, 2.07, 2.04, 2.03, 2.02, 2.015, 2.010, 2.00, 1.99 (s, 39H, 13 × Ac), 0.55−2.00 (m, 33H, 12 × CH_2, 9 × CH), 0.90 (d, 3H, J = 6.6, cholestanyl-CH_3), 0.871 (d, 3H, J = 6.6, cholestanyl-CH_3), 0.867 (d, 3H, J = 6.6, cholestanyl-CH_3), 0.78 (s, 3H, cholestanyl-CH_3), 0.65 (s, 3H, cholestanyl-CH_3).

3β-Cholestanyl α-D-Glucopyranosyl-(1→4)-α-D-glucopyranosyl-(1→4)-α-D-glucopyranosyl-(1→4)-β-D-glucopyranoside (33). The peracetate **32** (75 mg, 0.047 mmol) was dissolved in anhydrous MeOH (0.1 M) and treated with a solution of NaOMe in MeOH (1.35 M, 0.2−0.6 equiv). The mixture was stirred at room temperature for 3 h (monitored by TLC). Acidic resin AG-50W-X8 (H^+ form) was added to adjust to pH 6−7. The mixture was filtered, and the resin was rinsed with MeOH. The combined filtrate and washings were concentrated in vacuo and thoroughly dried to give the polyol **33** as a white solid (48 mg, 98%). ESMS m/z 1059.6 (M + Na^+); HR ESMS m/z 1059.5667 (M + Na^+, calcd for $C_{51}H_{88}O_{21}Na^+$ 1059.5710). Polyol **33** was analyzed by 1D and 2D NMR spectroscopy in DMSO-d_6 at 600 MHz and the ^{1}H and ^{13}C chemical shift data are presented in Tables S1 and S2. Chemical shifts were fully assigned using gHSQC, gCOSY, gHMBC, TOCSY, and ROESY techniques.

3β-Cholestanyl 2,3,4,6-Tetra-*O*-sulfo-α-D-glucopyranosyl-(1→4)-2,3,6-tri-*O*-sulfo-α-D-glucopyranosyl-(1→4)-2,3,6-tri-*O*-sulfo-α-D-glucopyranosyl-(1→4)-2,3,6-tri-*O*-sulfo-β-D-glucopyranoside, Tridecasodium Salt (18, PG545). The polyol **33** (48 mg, 0.046 mmol) was dissolved in dry DMF (2.3 mL, 0.02 M) and freshly washed and dried SO_3−pyridine complex (285 mg, 3 equiv per OH group, 1.79 mmol) added, and the mixture was stirred at 60 °C for 16 h. The reaction mixture was cooled to 0 °C for 10 min, then neutralized by adding ice-cold aqueous NaOH solution (5 M, 2.1 equiv/SO_3, 0.752 mL, 3.76 mmol) at 0 °C in one portion (to pH 12). The suspension was stirred at 0 °C for 15 min, diluted with water (10 mL), and concentrated in vacuo at 40 °C. A pale yellow powder was afforded, which was dissolved in water (10 mL), obtaining a solution with pH 11.5. The solution was set to pH 12.5 by adding an aqueous solution of NaOH (5 M, 5 drops) and dialyzed against water (4 L) using a Slide-A-Lyzer cassette (2000 MWCO, 4−12 mL) for 16 h at room temperature. The dialysis against water (4 L) was continued at 0 °C for 3 days, whereby the water was changed after each 24 h, as well as an aqueous solution NH_4HCO_3 (3 M, 0.6 mL) was added to the water to set the pH to ∼6.0−6.5. The desalted solution was then lyophilized to afford the polysulfate **18** as a white fluffy powder (97 mg, 89%, 99% pure by CE[20]). ^{1}H NMR (400 MHz, D_2O): δ 5.63 (d, 1 H, $J_{1,2}$ = 3.3, H1), 5.60 (d, 1 H, $J_{1,2}$ = 3.6, H1), 5.50 (d, 1H, $J_{1,2}$ = 3.6, H1), 5.01 (d, 1H, $J_{1,2}$ = 4.8, H1^{I}), 4.10−4.93 (m, 23H, 4 × H2, 4 × H3, 4 × H-4, 3 × H5, 8 × H6), 4.05 (m, 1H, H5^{I}), 3.76 (m, 1 H, H-3 chol), 0.54−1.97 (m, 33 H, 12 × CH_2, 9 × CH), 0.86 (d, 3H, J = 6.5, cholestanyl-CH_3), 0.795 (d, 3H, J = 6.6, cholestanyl-CH_3), 0.792 (d, 3H, J = 6.6, cholestanyl-CH_3), 0.76 (s, 3H, cholestanyl-CH_3), 0.61 (s, 3H, cholestanyl-CH_3). Polysulfate **18** was also analyzed by 1D and 2D NMR spectroscopy in D_2O at 600 MHz, and the ^{1}H and ^{13}C chemical shift data are presented in Tables S3 and S4. Chemical shifts were fully assigned using gHSQC, gCOSY, gHMBC, TOCSY, and ROESY techniques.

Biological Assays. Growth Factor Binding Assays. The binding affinities of the compounds for the growth factors FGF-1, FGF-2, and VEGF were determined on a BIAcore 3000 (BIAcore, Uppsala, Sweden) using a surface plasmon resonance-based solution affinity assay, as previously described.[21,22] Heparin-coated CM4 sensor chips were prepared via reductive amination of the reducing end aldehyde with 1,4-diaminobutane, as previously described.[22] Ligands binding to FGF-1 and VEGF were measured in HBS-EP buffer (10 mM HEPES, pH 7.4, 150 mM NaCl, 3.0 mM EDTA, and 0.005% (v/v) polysorbate 20), while binding to FGF-2 was measured in HBS-EP buffer containing 300 mM NaCl. Sensorgram data were analyzed using the BIAevaluation software, version 4.1 (BIAcore), and K_d values were determined as previously described.[22] The K_d values represent the average of at least duplicate measurements ± SD. The data are presented in Table 1.

Heparanase Inhibition Assay. The inhibitory potency of the test compounds against recombinant human heparanase was determined by the fondaparinux assay as previously described.[23] Briefly, assay solutions (100 μL) comprised 40 mM sodium acetate buffer, pH 5.0, 100 mM fondaparinux (GlaxoSmithKline) with or without inhibitor. Heparanase was added to a final concentration of 140 pM to start the assay. The plates were sealed with adhesive tape and incubated at 37 °C for 2−24 h before the assays were stopped by the addition of 100 μL of a solution containing 1.69 mM 4-[3-(4-iodophenyl)-2-(4-nitrophenyl)-2*H*-5-tetrazolio]-1,3-benzene disulfonate (WST-1, Auspep, Melbourne, Australia) in 0.1 M NaOH. The plates were resealed with adhesive tape and developed at 60 °C for 60 min, and the absorbance was measured at 584 nm (Fluostar, BMG Labtech). In each plate, a standard curve constructed with D-galactose as the reducing sugar standard was prepared in the same buffer and volume over the range of 2−100 μM. The IC_{50} value was determined and converted to a K_i using the method of Cheng and Prusoff.[35] All curve fitting was done using BIAevaluation software, version 4.1 (Biacore).

Growth Factor Induced Endothelial Cell Proliferation Assay. Endothelial cell culture using HUVEC cells was carried out as previously described.[16] Test compounds were weighed out from powder stocks and diluted in PBS to 10 mM stock solutions and stored at −80 °C. For experiments, compounds were subsequently diluted in EBM-2 medium (supplemented with 2% FBS and gentamicin) to various working concentrations as required. The proliferation assays using various concentrations of the growth factor VEGF, FGF-1, or FGF-2 were carried out as previously described.[16] Briefly, 100 μL of cells was added to each well at concentrations between 1 × 10^3 and 3 × 10^3 per well. Growth factors and test compounds were then added in 50 μL volumes at specified concentrations (typically seven ranging from 1−50 μM in triplicate) to obtain a final volume of 200 μL. Following incubation for 70 h, 20 μL of the CellTiter 96 Aqueous One solution cell proliferation assay (Promega) was added for 2 h prior to reading the absorbance at 490 nm to obtain OD values. Once these values were subtracted from the blanks (media only), the data were imported into BIAevaluation

software to determine IC_{50} values for each curve. The IC_{50} data represent the mean and standard deviation to indicate the interexperimental error where compounds were tested in two to eight independent experiments. Data without SD are from single experiments.

Matrigel Microtubule Formation Assay. The tube formation assay was performed as described previously.[25] Briefly, HUVECs in the fourth or fifth passage at 70−80% confluence were harvested and resuspended in Lonza endothelial growth medium (EGM2) containing all supplements as directed by the manufacturer, except heparin, at a cell density of 4×10^5 cells per mL. For each set of triplicate wells, an amount of 200 μL of cells (4×10^5/mL) was treated with an equal volume of compound to obtain a final concentration of 10, 50, or 100 μM (thus ensuring 1×300 μL is available for each condition). A 100 μL aliquot of cells was then plated onto 96-well plates precoated with growth factor reduced Matrigel (50 μL for 30 min followed by a further 30 μL for 1 h) and incubated for 18 h. Tube formation was examined by phase-contrast microscopy, and images were collected using an Olympus C5050 digital camera. Tube formation inhibition was quantified manually from images by recording the total number of branching nodes connecting three or more tubules. Results are expressed as percentage inhibition compared to control (untreated HUVECs were used as a control for normal cell growth and tube formation in Matrigel).

Ex Vivo Rat Aortic Angiogenesis Assay. The ex vivo rat aortic angiogenesis assay was carried out as previously described.[16,29] Briefly, rat aortas were harvested from 6 to 10 week old Sprague−Dawley rats by Tetra-Q, Brisbane, Australia, and trimmed of remaining fat and connective tissue before cutting 1 mm ring sections which were subsequently bisected and transferred to complete EBM-2 medium (Lonza, Basel, Switzerland) containing 2% FCS and all SingleQuot reagents except for heparin. Matrigel (BD Biosciences, San Jose, CA, U.S.) was allowed to cool on ice, and once in a liquid form, 180 μL was pipetted into 48-well tissue culture plates (Nunc, Rochester, NY, U.S.). The plates were incubated at 37 °C for 30 min to allow Matrigel to solidify. Aortic segments were then carefully placed on top on the Matrigel in the center of each well, and 60 μL of Matrigel was pipetted to cover the aortic segment. The plate was then returned to the incubator for a further 20 min before each well was supplemented with 1.0 mL of medium in the absence (control) or presence of test compounds usually at two concentrations within the range of 1−50 μM (test compound stock solutions (10 mM) were prepared using sterile phosphate buffered saline, pH 7.2), depending on the particular compound/experiment. Cultures were replenished as appropriate every 48 h, and scoring of microvessels (from 0 [least] to 5 [most positive]) was carried out at various time points up to 8 days by two investigators in an independent fashion as previously described.[36] Sprouting vessels were photographed using the 4× objective with an Olympus C-7070 camera and an adaptor for the eyepiece. In some instances, to determine the potential toxicity of compounds in this assay, the viability of the tissue was assessed by withdrawing the compound/medium from the culture on day 6 or 7 and adding complete medium with VEGF (typically 10 ng/mL) for up to an additional 7 days. In the absence of toxicity, the viable tissue should sprout microvessels in response to the exogenous growth factor.

Anticoagulant Activity Assays. The anticoagulant activity of the test compounds was determined by measuring the effect of various concentrations of compound (0−100 μg/mL in PBS) on the elevation of the APTT of pooled normal human plasma. Clotting assays were performed with a ball coagulameter KC10 (Amelung, Lemgo, Germany) using standard protocols according to the manufacturer's instructions. Unfractionated heparin (UFH) was used as the control. The normal range of APTT for pooled normal human plasma is 26−36 s. The coefficient of variation for APTT coagulation values of 36 s is 2%, and for coagulation values of 90 s and higher it is 5−7%. The compounds were also evaluated in the Heptest as previously described.[16] Heptest values in normal plasma samples ranged from 13 to 20 s (mean, 17.1 ± 2.1 s). The coefficient of variation for Heptest coagulation values is 1.8% for values of 20−90 s and 3−4% for values above 90 s.

Preliminary Pharmacokinetic Analyses for Compounds 18, 23, 24. Male Sprague−Dawley rats (250−350 g) were obtained from the Herston Medical Research Centre at Royal Brisbane Hospital, Australia. The animals were allowed free access to food and water before and during the experiment, during which they were maintained unrestrained in metabolism cages. Animal procedures were approved by The University of Queensland Animal Ethics Committee. Rats were anesthetized with isoflurane (Forthane). A catheter was inserted in the external jugular vein via an incision in the neck and was passed under the skin to a second incision in the skin of the back (midline vicinity of the scapulae). This was then exteriorized with the protection of a light metal spring. The incision was closed and the spring fixed to the skin with Michel sutures so that the rats had a full range of movement. The animals were carefully monitored during recovery (1 h). The dose was prepared in phosphate-buffered saline to give a total drug concentration of 5.00 mg/mL. All doses were administered as a bolus of 10 mg/kg in a dose volume of approximately 2 mL/kg. Blood samples (about 250 μL) were collected predose and at 5, 10, 20, 35, 65, 125, 185, 305, and 455 min after dosing. The blood samples were immediately centrifuged, and an aliquot of the plasma was transferred to a vial for CE analysis. At completion of the experiments, the animals were sacrificed by a lethal overdose of iv pentobarbitone.

Sample Preparation. Rat plasma samples (100 μL) were mixed with 25 μL of 1% SDS and 75 μL of 5% CHAPS. Proteinase K solution (50 μL of 40 mg/mL in 5 mM $CaCl_2$) was added, and the mixture was incubated at 37 °C for 1.5 h and then sonicated at 40 °C for 60 min. An additional 230 μL of water was added to the sample solution, and this was transferred onto a preconditioned (MeOH × 1 mL, water × 1 mL, 0.1 M NH_4Ac × 1 mL) Waters Oasis WAX cartridge (30 μm, 1 mL/30 mg). The WAX cartridge was washed with 0.1 M NH_4OAc (1 mL) followed by water (1 mL), 2% acetic acid (1 mL), water (1 mL), MeOH (3 mL), and finally water (1 mL). The product was eluted off the cartridge using ammonia solution [prepared by mixing 28% NH_3 solution (18 mL) with 1:1 MeOH−water (32 mL)], and the solution was freeze-dried and redissolved into 200 μL of water for CE analysis.

CE Analysis. Samples were analyzed by CE in reverse polarity mode on an Agilent HP^{3D} CE system equipped with a DAD detector. Beckman eCap fused silica capillaries (75 μm i.d., 375 μm o.d., 66 cm total length, 57.5 cm to detector) were used in these analyses. Indirect UV detection was used relying on 10 mM 5-sulfosalicylic acid, pH 3.0 (adjusted with aqueous NaOH), as the background electrolyte with detection at 214 nM. The capillary temperature was 20 °C, and the operating voltage was −25 kV. Samples were injected using electrokinetic supercharging (−10 kV, 200 s) for online preconcentration. The limit of detection for **18** was 20 μg/mL.

Data Analysis. Plasma concentration versus time curves were plotted (see Supporting Information), and apparent pharmacokinetic parameters were estimated from the notionally linear portion of the curve. The apparent terminal elimination half-lives ($t_{1/2}$) for **18**, **23**, and **24** were estimated to be 7.19, 5.86, and 5.89 h, respectively.

■ ASSOCIATED CONTENT

Ⓢ Supporting Information

Experimental procedures and characterization data for selected compounds; tables of ^1H and ^{13}C NMR chemical shift assignments for compounds **33** and **18**; plots of mean plasma concentration versus time for compounds **18**, **23**, and **24**; ^1H NMR spectra for compounds **30**, **32**, **33**, and **18**; capillary electropherograms for sulfonated test compounds. This material is available free of charge via the Internet at http://pubs.acs.org.

■ AUTHOR INFORMATION

Corresponding Author

*Phone, +617-3346 9598; fax, +617-3365 4299; e-mail, v.ferro@uq.edu.au.

Present Addresses

[§]School of Chemistry and Molecular Biosciences, The University of Queensland, Brisbane, Queensland 4072, Australia.
[∥]Institute for Molecular Bioscience, The University of Queensland, Brisbane, Qld 4072, Australia.
[⊥]National Food Technology Research Centre, Kanye, Botswana.
[#]Alchemia Ltd., Eight Mile Plains, Queensland 4113, Australia.
[∞]QLD Health Forensic and Scientific Services, Coopers Plains, Queensland 4108, Australia.
[¶]Eskitis Institute for Cell and Molecular Therapies, Griffith University, Nathan Qld 4111, Australia.

Notes

The authors declare no competing financial interest.

■ ACKNOWLEDGMENTS

We thank Tony Carroll for high field NMR analysis of **18** and **33**, Karine Mardon, Russell Addison, Edmund Kostewicz, William Charman, and Tom Gonda for assistance with pharmacokinetic and in vivo studies, and David Hume, Keith Watson, Ron Dickinson, and Jeremy Turnbull for useful discussions.

■ ABBREVIATIONS USED

HS, heparan sulfate; VEGF, vascular endothelial growth factor; FGF, fibroblast growth factor; HUVEC, human umbilical vein endothelial cell; dHMVEC, dermal human microvascular endothelial cell; APTT, activated partial thromboplastin time; PBS, phosphate buffered saline; TKI, tyrosine kinase inhibitor

■ REFERENCES

(1) Ferrara, N.; Kerbel, R. S. Angiogenesis as a therapeutic target. *Nature* **2005**, *438*, 967−974.
(2) Folkman, J. Angiogenesis: an organizing principle for drug discovery? *Nat. Rev. Drug Discovery* **2007**, *6*, 273−286.
(3) Herbst, R. S. Therapeutic options to target angiogenesis in human malignancies. *Expert Opin. Emerging Drugs* **2006**, *11*, 635−650.
(4) Bergers, G.; Hanahan, D. Modes of resistance to anti-angiogenic therapy. *Nat. Rev. Cancer* **2008**, *8*, 592−603.
(5) Casanovas, O.; Hicklin, D. J.; Bergers, G.; Hanahan, D. Drug resistance by evasion of antiangiogenic targeting of VEGF signaling in late-stage pancreatic islet tumors. *Cancer Cell* **2005**, *8*, 299−309.
(6) Paez-Ribes, M.; Allen, E.; Hudock, J.; Takeda, T.; Okuyama, H.; Vinals, F.; Inoue, M.; Bergers, G.; Hanahan, D.; Casanovas, O. Antiangiogenic therapy elicits malignant progression of tumors to increased local invasion and distant metastasis. *Cancer Cell* **2009**, *15*, 220−231.
(7) Ebos, J. M.; Lee, C. R.; Cruz-Munoz, W.; Bjarnason, G. A.; Christensen, J. G.; Kerbel, R. S. Accelerated metastasis after short-term treatment with a potent inhibitor of tumor angiogenesis. *Cancer Cell* **2009**, *15*, 232−239.
(8) Loges, S.; Mazzone, M.; Hohensinner, P.; Carmeliet, P. Silencing or fueling metastasis with VEGF inhibitors: antiangiogenesis revisited. *Cancer Cell* **2009**, *15*, 167−170.
(9) Force, T.; Kolaja, K. L. Cardiotoxicity of kinase inhibitors: the prediction and translation of preclinical models to clinical outcomes. *Nat. Rev. Drug Discovery* **2011**, *10*, 111−126.
(10) Casu, B.; Vlodavsky, I.; Sanderson, R. D. Non-anticoagulant heparins and inhibition of cancer. *Pathophysiol. Haemostasis Thromb.* **2008**, *36*, 195−203.
(11) Hammond, E.; Bytheway, I.; Ferro, V. Heparanase as a Target for Anticancer Therapeutics: New Developments and Future Prospects. In *New Developments in Therapeutic Glycomics*; Delehedde, M., Lortat-Jacob, H., Eds.; Research Signpost: Trivandrum, India, 2006; pp 251−282.
(12) McKenzie, E. A. Heparanase: a target for drug discovery in cancer and inflammation. *Br. J. Pharmacol.* **2007**, *151*, 1−14.
(13) Parish, C. R.; Freeman, C.; Brown, K. J.; Francis, D. J.; Cowden, W. B. Identification of sulfated oligosaccharide-based inhibitors of tumor growth and metastasis using novel in vitro assays for angiogenesis and heparanase activity. *Cancer Res.* **1999**, *59*, 3433−3441.
(14) Liu, C. J.; Lee, P. H.; Lin, D. Y.; Wu, C. C.; Jeng, L. B.; Lin, P. W.; Mok, K. T.; Lee, W. C.; Yeh, H. Z.; Ho, M. C.; Yang, S. S.; Lee, C. C.; Yu, M. C.; Hu, R. H.; Peng, C. Y.; Lai, K. L.; Chang, S. S.; Chen, P. J. Heparanase inhibitor PI-88 as adjuvant therapy for hepatocellular carcinoma after curative resection: a randomized phase II trial for safety and optimal dosage. *J. Hepatol.* **2009**, *50*, 958−968.
(15) Recent review: Kudchadkar, R.; Gonzalez, R.; Lewis, K. D. PI-88: a novel inhibitor of angiogenesis. *Expert Opin. Invest. Drugs* **2008**, *17*, 1769−1776.
(16) Johnstone, K. D.; Karoli, T.; Liu, L.; Dredge, K.; Copeman, E.; Li, C. P.; Davis, K.; Hammond, E.; Bytheway, I.; Kostewicz, E.; Chiu, F. C.; Shackleford, D. M.; Charman, S. A.; Charman, W. N.; Harenberg, J.; Gonda, T. J.; Ferro, V. Synthesis and biological evaluation of polysulfated oligosaccharide glycosides as inhibitors of angiogenesis and tumor growth. *J. Med. Chem.* **2010**, *53*, 1686−1699.
(17) Wall, D.; Douglas, S.; Ferro, V.; Cowden, W.; Parish, C. Characterisation of the anticoagulant properties of a range of structurally diverse sulfated oligosaccharides. *Thromb. Res.* **2001**, *103*, 325−335.
(18) Karoli, T.; Liu, L.; Fairweather, J. K.; Hammond, E.; Li, C. P.; Cochran, S.; Bergefall, K.; Trybala, E.; Addison, R. S.; Ferro, V. Synthesis, biological activity, and preliminary pharmacokinetic evaluation of analogues of a phosphosulfomannan angiogenesis inhibitor (PI-88). *J. Med. Chem.* **2005**, *48*, 8229−8236.
(19) Ferro, V.; Dredge, K.; Liu, L.; Hammond, E.; Bytheway, I.; Li, C.; Johnstone, K.; Karoli, T.; Davis, K.; Copeman, E.; Gautam, A. PI-88 and novel heparan sulfate mimetics inhibit angiogenesis. *Semin. Thromb. Hemostasis* **2007**, *33*, 557−568.
(20) Yu, G.; Gunay, N. S.; Linhardt, R. J.; Toida, T.; Fareed, J.; Hoppensteadt, D. A.; Shadid, H.; Ferro, V.; Li, C.; Fewings, K.; Palermo, M. C.; Podger, D. Preparation and anticoagulant activity of the phosphosulfomannan PI-88. *Eur. J. Med. Chem.* **2002**, *37*, 783−791.
(21) Cochran, S.; Li, C.; Fairweather, J. K.; Kett, W. C.; Coombe, D. R.; Ferro, V. Probing the interactions of phosphosulfomannans with angiogenic growth factors by surface plasmon resonance. *J. Med. Chem.* **2003**, *46*, 4601−4608.
(22) Cochran, S.; Li, C. P.; Ferro, V. A surface plasmon resonance-based solution affinity assay for heparan sulfate-binding proteins. *Glycoconjugate J.* **2009**, *26*, 577−587.
(23) Hammond, E.; Li, C. P.; Ferro, V. Development of a colorimetric assay for heparanase activity suitable for kinetic analysis and inhibitor screening. *Anal. Biochem.* **2010**, *396*, 112−116.
(24) Note that this assay uses fondaparinux as substrate rather than HS and no BSA carrier to stabilize the enzyme. The resultant K_i values are approximately 20-fold lower than with HS-based assays which require BSA and result in compound loss due to binding to BSA.
(25) Dredge, K.; Hammond, E.; Davis, K.; Li, C. P.; Liu, L.; Johnstone, K.; Handley, P.; Wimmer, N.; Gonda, T. J.; Gautam, A.; Ferro, V.; Bytheway, I. The PG500 series: novel heparan sulfate mimetics as potent angiogenesis and heparanase inhibitors for cancer therapy. *Invest. New Drugs* **2010**, *28*, 276−283.
(26) Fairweather, J. K.; Hammond, E.; Johnstone, K. D.; Ferro, V. Synthesis and heparanase inhibitory activity of sulfated mannooligosaccharides related to the antiangiogenic agent PI-88. *Bioorg. Med. Chem.* **2008**, *16*, 699−709.
(27) Tornøe, C. W.; Christensen, C.; Meldal, M. Peptidotriazoles on solid phase: [1,2,3]-triazoles by regiospecific copper(I)-catalyzed 1,3-dipolar cycloadditions of terminal alkynes to azides. *J. Org. Chem.* **2002**, *67*, 3057−3064.
(28) Rostovtsev, V. V.; Green, L. G.; Fokin, V. V.; Sharpless, K. B. A stepwise Huisgen cycloaddition process: copper(I)-catalyzed regioselective

"ligation" of azides and terminal alkynes. *Angew. Chem., Int. Ed.* **2002**, *41*, 2596−2599.
(29) Liu, L.; Johnstone, K.; Fairweather, J. K.; Dredge, K.; Ferro, V. An improved synthetic route to the potent angiogenesis inhibitor benzyl manα(1→3)-manα(1→3)-manα(1→3)-manα(1→2)-man hexadecasulfate. *Aust. J. Chem.* **2009**, *62*, 546−552.
(30) Subsequent treatment with NaOMe in MeOH to remove acyl groups prior to sulfonation failed to remove the C-12 acetyl group from deoxycholic acid.
(31) Reviews: (a) Imberty, A.; Lortat-Jacob, H.; Pérez, S. Structural view of glycosaminoglycan−protein interactions. *Carbohydr. Res.* **2007**, *342*, 430−439. (b) Coombe, D. R.; Kett, W. C. Heparan sulfate−protein interactions: therapeutic potential through structure−function insights. *Cell. Mol. Life Sci.* **2005**, *62*, 410−424. (c) Raman, R.; Sasisekharan, V.; Sasisekharan, R. Structural insights into biological roles of protein−glycosaminoglycan interactions. *Chem. Biol.* **2005**, *12*, 267−277. (d) Capila, I.; Linhardt, R. J. Heparin−protein interactions. *Angew. Chem., Int. Ed.* **2002**, *41*, 391−412.
(32) Auerbach, R.; Lewis, R.; Shinners, B.; Kubai, L.; Akhtar, N. Angiogenesis assays: a critical overview. *Clin. Chem.* **2003**, *49*, 32−40.
(33) Dredge, K.; Hammond, E.; Handley, P.; Gonda, T. J.; Smith, M. T.; Vincent, C.; Brandt, R.; Ferro, V.; Bytheway, I. PG545, a dual heparanase and angiogenesis inhibitor, induces potent anti-tumour and anti-metastatic efficacy in preclinical models. *Br. J. Cancer* **2011**, *104*, 635−642.
(34) Narumi, A.; Miura, Y.; Otsuka, I.; Yamane, S.; Kitajyo, Y.; Satoh, T.; Hirao, A.; Kaneko, N.; Kaga, H.; Kakuchi, T. End-functionalization of polystyrene by malto-oligosaccharide generating aggregation-tunable polymeric reverse micelle. *J. Polym. Sci., Part A: Polym. Chem* **2006**, *44*, 4864−4879.
(35) Cheng, Y.; Prusoff, W. H. Relationship between the inhibition constant (K1) and the concentration of inhibitor which causes 50 per cent inhibition (I50) of an enzymatic reaction. *Biochem. Pharmacol.* **1973**, *22*, 3099−3108.
(36) Min, J. K.; Han, K. Y.; Kim, E. C.; Kim, Y. M.; Lee, S. W.; Kim, O. H.; Kim, K. W.; Gho, Y. S.; Kwon, Y. G. Capsaicin inhibits in vitro and in vivo angiogenesis. *Cancer Res.* **2004**, *64*, 644−651.